Large eddy simulations of miscible Rayleigh-Taylor instability

T. W. Mattner and P. E. Dimotakis

Introduction

Rayleigh-Taylor (RT) instability occurs when fluids of different density are subject to an acceleration-induced pressure gradient opposite in direction to the density gradient. The instability is driven by buoyancy forces due to local density variations. Direct numerical simulations (DNS) of miscible RT instability are unable to settle basic questions concerning growth-rate because resolution limitations prevent sufficiently high Reynolds numbers or self-similarity from being attained. The purpose of this paper is to apply the stretched-vortex model to large eddy simulation (LES) of RT instability, and compare these with DNS results.

Governing equations

The equations of motion are obtained by Favre-filtering those used in the direct numerical simulations of Cook & Dimotakis[1]. The Favre-filter is defined by

$$\widetilde{f} \equiv \frac{\overline{\rho f}}{\overline{\rho}}, \tag{1}$$

where f is any field, ρ the density,

$$\overline{f} \equiv \int G(\boldsymbol{x}-\boldsymbol{x}')f(\boldsymbol{x}')\,\mathrm{d}\boldsymbol{x}', \tag{2}$$

$\boldsymbol{x}$ the spatial coordinate vector, and G the filter function. The fluids are assumed to be incompressible and the density variable due to changes in mixture composition. The Favre-filtered heavy-fluid mass-fraction, $\widetilde{Y}$, and the filtered heavy-fluid mole-fraction, $\overline{X}$, are related to the filtered density, $\overline{\rho}$, by

$$\frac{1}{\overline{\rho}} = \frac{\widetilde{Y}}{\rho_2} + \frac{1-\widetilde{Y}}{\rho_1} \quad \text{and} \quad \overline{X} = \frac{\overline{\rho}-\rho_1}{\rho_2-\rho_1}, \tag{3}$$

where ρ_1 and ρ_2 are the light- and heavy-fluid densities, respectively. The Favre-filtered continuity, species-transport, and momentum equations are

$$\frac{\partial\overline{\rho}}{\partial t} + \frac{\partial\overline{\rho}\widetilde{u}_j}{\partial x_j} = 0, \tag{4a}$$

$$\frac{\partial\overline{\rho}\widetilde{Y}}{\partial t} + \frac{\partial\overline{\rho}\widetilde{u}_j\widetilde{Y}}{\partial x_j} = \frac{\partial}{\partial x_j}\left(\overline{\rho\mathcal{D}\frac{\partial Y}{\partial x_j}}\right) - \frac{\partial\overline{\rho}q_j}{\partial x_j}, \tag{4b}$$

$$\frac{\partial\overline{\rho}\widetilde{u}_i}{\partial t} + \frac{\partial\overline{\rho}\widetilde{u}_i\widetilde{u}_j}{\partial x_j} = -\frac{\partial\overline{p}}{\partial x_i} + \frac{\partial\overline{\tau}_{ij}}{\partial x_j} - \overline{\rho}g\delta_{i3} - \frac{\partial\overline{\rho}T_{ij}}{\partial x_j}, \tag{4c}$$

where $\mathcal{D}$ is the diffusivity, p the pressure, τ_{ij} the viscous stress tensor, g the acceleration, q_j the subgrid-scale (SGS) scalar flux, and T_{ij} the SGS stress tensor. Equations (3), (4a), and (4b) imply

$$\frac{\partial\widetilde{u}_j}{\partial x_j} = -\frac{\partial}{\partial x_j}\left(\overline{\frac{\mathcal{D}}{\rho}\frac{\partial\rho}{\partial x_j}}\right) - \left(\frac{1}{\rho_2}-\frac{1}{\rho_1}\right)\frac{\partial\overline{\rho}q_j}{\partial x_j} \tag{5}$$

and this constraint is used instead of (4b).

Equations (4a), (4c), and (5) are closed using the stretched-vortex SGS stress model of Misra & Pullin[2] and the stretched-vortex SGS passive scalar mixing model of Pullin[3]. These uniform-density models are adpated to the variable-density case following Kosovic *et al.*[4]. For a single subgrid vortex, the SGS stress is

$$T_{ij} = K(\delta_{ij} - e_i e_j) \tag{6}$$

where K is the subgrid kinetic energy per unit mass, and $\boldsymbol{e} = (e_1, e_2, e_3)$ is the unit vector of the subgrid vortex axis. The SGS scalar flux is

$$q_j = -\frac{1}{2}\Delta K^{1/2}(\delta_{ij} - e_i e_j)\frac{\partial\widetilde{Y}}{\partial x_i} \tag{7}$$

where Δ is the local mesh size. Together with (3) and (5), this implies

$$\frac{\partial\widetilde{u}_j}{\partial x_j} = -\frac{\partial}{\partial x_j}\left(\frac{\mathcal{D}}{\overline{\rho}}\frac{\partial\overline{\rho}}{\partial x_j}\right) - \frac{\partial}{\partial x_j}\left[\frac{1}{2}\Delta K^{1/2}(\delta_{ij}-e_ie_j)\frac{1}{\overline{\rho}}\frac{\partial\overline{\rho}}{\partial x_i}\right]. \tag{8}$$

The diffusive (and viscous stress) term is written such that the original unfiltered equation is recovered when contributions from the model are small. In our numerical scheme, the divergence of the Favre-filtered velocity is used in the solution of a variable-coefficient elliptic equation for the filtered pressure. K is estimated from a prescribed energy spectrum, either $E(k) = \mathcal{K}_0\epsilon^{2/3}k^{-5/3}$ (Kolmogorov spectrum without viscous cutoff) or $E(k) = \mathcal{K}_0\epsilon^{2/3}k^{-5/3}\exp[-2k^2\nu/(3|a|)]$ (Lundgren spiral spectrum), where k is the wavenumber, $\mathcal{K}_0$ the Kolmogorov prefactor, ϵ the local cell-averaged dissipation rate, ν the kinematic viscosity, and $|a|$ the axial strain along the subgrid vortex axis.[4,5] The group $\mathcal{K}_0\epsilon^{2/3}$ is estimated from the local second-order velocity structure function using circular averages in the homogeneous plane.[5] The proportion of subgrid vortices aligned with the principal extensional eigenvector of the resolved rate-of-strain tensor, $\widetilde{S}_{ij}$, and the resolved vorticity vector, $\boldsymbol{\omega}$, is given by λ and $(1-\lambda)$, respectively, where $\lambda = \lambda_3/(\lambda_3 + ||\boldsymbol{\omega}||)$ and λ_3 is the principal extensional eigenvalue (model 1b[2]).

Results

Figure 1 shows a constant mole-fraction isosurface from a $128^2 \times 512$ LES of miscible RT instability, at a

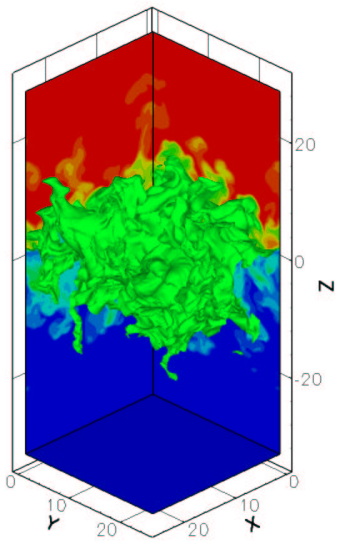

Fig. 1 $\overline{X} = 1/2$ **isosurface at a density ratio** $\rho_2/\rho_1 = 3$**. Red indicates heavy-fluid (**$\overline{X} = 1$**) and blue light-fluid (**$\overline{X} = 0$**).**

density-ratio of 3. The acceleration is in the vertical direction. The top and bottom of the domain are no-slip walls, and the transverse homogeneous plane is periodic. This simulation uses the unbounded Kolmogorov spectrum for the subgrid energy. The Reynolds number is about 18,000, where the Reynolds number is defined by the thickness of the mixing zone, its rate of growth, the arithmetic mean density and the viscosity. For comparison, the highest Reynolds number obtained by DNS is around 5,500 on a $512^2 \times 2040$ grid.[6]

In this example, the density field exhibits small-amplitude ($\sim$ 1% ρ_1) high-wavenumber under/overshoots ($\overline{\rho} < \rho_1$ or $\overline{\rho} > \rho_2$) which are, however, unphysical. In the implmentation described here, the excursions are controlled by means of a circular spectral filter in the homogeneous plane, and a compact Pade filter in the vertical inhomogeneous direction. The filters are used to control wavenumbers in the range $k > k_c$, where $k_c = \pi/\Delta$ is the model cutoff wavenumber. Without such filtering, the amplitude of the excursions may grow to as large as 10% ρ_1.

Figure 2 shows mixing-zone growth as measured by the bubble and spike heights, h_B and h_S, respectively. These are defined in terms of the lateral average filtered mole-fraction, $\langle\overline{X}\rangle$, which is a function of the vertical coordinate, z, as $\langle\overline{X}\rangle(z = h_\mathrm{B}) = 0.99$ and $\langle\overline{X}\rangle(z = h_\mathrm{S}) = 0.01$. In the absence of externally imposed length-scales, and at sufficiently large Reynolds number, classic dimensional analysis suggests the growth will be quadratic. In this example, bubble growth is almost linear.

Performance of the model is assessed by comparison of coarse resolution LES against fully-resolved DNS

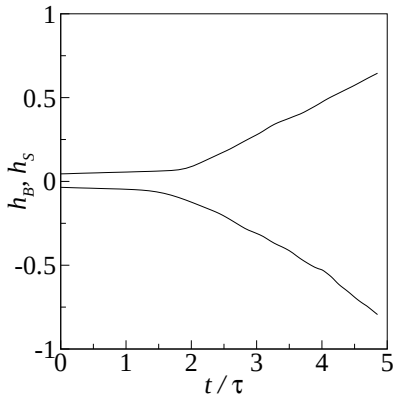

Fig. 2 Mixing-zone growth. $h_\mathrm{B} > 0$**,** $h_\mathrm{S} < 0$**.** $\tau = \sqrt{L/\mathcal{A}g}$**, where** L **is the lateral dimension of the computational domain and** $\mathcal{A} = (\rho_2 - \rho_1)/(\rho_2 + \rho_1)$**.**

at three density-ratios: 5/3, 3, and 7. The initial conditions for the LES are obtained by filtering the DNS data at a time when the mixing-zone has grown sufficiently thick to be represented on the coarse LES grid. The Reynolds numbers for these tests are limited to less than 4,000. Statistics for comparison include mixing-zone width, mole-fraction mean and variance, kinetic energy and dissipation rate, and spectra.

Acknowledgements

We gratefully acknowledge the help of D. I. Pullin in implementing the subgrid vortex model and A. W. Cook for supplying the DNS code on which the current LES implementation is based.

References

[1] A. W. Cook and P. E. Dimotakis. Transition stages of Rayleigh-Taylor instability between miscible fluids. *J. Fluid Mech.*, 443:69–99, 2001.

[2] A. Misra and D. I. Pullin. A vortex-based subgrid stress model for large-eddy simulation. *Phys. Fluids*, 9:2443–2454, 1997.

[3] D. I. Pullin. A vortex-based model for the subgrid flux of a passive scalar. *Phys. Fluids*, 12:2311–2319, 2000.

[4] B. Kosovic, D. I. Pullin, and R. Samtaney. Subgrid-scale modeling for large-eddy simulations of compressible turbulence. *Phys. Fluids*, 14:1511–1522, 2002.

[5] T. Voekl, D. I. Pullin, and D. C. Chan. A physical-space version of the stretched-vortex subgrid-stress model for large-eddy simulation. *Phys. Fluids*, 12:1810–1825, 2000.

[6] A. W. Cook and Y. Zhou. Energy transfer in Rayleigh-Taylor instability. *Phys. Rev. E*, 66, 2002.